communications biology

A Nature Portfolio journal

Article

Article in Press

https://doi.org/10.1038/s42003-026-11053-7

Short-term exposure to different thermal variability regimes does not shift heatwave tolerance in tropical calcifying macroalgae

Check for updates

Erik C. Krieger ✉, Lauren Tisdale, Fleur C. Bruggemann, Lena Y. Li, Gage Mele, Huajing Yan, Walter Rich & Maggie D. Johnson ✉

Exposure to fluctuating seawater temperatures can increase the physiological tolerance of some marine organisms to heatwaves. Yet, if thermal variability similarly influences the tolerances of key calcifying taxa, such as reef-building algae, remains unresolved. We experimentally tested whether diurnal temperature variability enhances heatwave tolerance in four species of tropical calcifying algae (*Halimeda opuntia*, *Halimeda discoidea*, *Neogoniolithon* sp. and *Lithophyllum* sp.), and whether responses differ depending on the occurrence of peak temperatures during the day versus the night. Heatwave exposure suppressed calcification and photophysiological performance in three of the four species, and neither temperature variability, nor the timing of peak thermal exposure, significantly altered this response. The thermal tolerance of the study species may, therefore, be rooted in their long-term environmental history, rather than short-term exposure to different variability regimes. The metabolic suppression induced by the heatwave demonstrates a poorly understood degree of vulnerability in this functional group. Despite these impacts, the algal species demonstrated greater resilience to heat stress than many reef-building corals likely would under equivalent conditions (7–10 Degree Heating Weeks). Differential thermal susceptibility among reef-building taxa, including potentially greater resilience in some algal species, may strongly influence the ecological trajectories of tropical reef communities as heatwaves increase in frequency and intensity.

Calcifying macroalgae are essential for maintaining healthy coral reef ecosystems[1–3]. Services provided by this important functional group include facilitation of coral larval settlement, reef framework stabilization and the production of sediment and carbonate[4–6], thereby contributing substantially to reef recovery, accretion and global carbonate cycling. Indeed, algal carbonate production can equal, or even surpass, that of reef-building corals, particularly after mass bleaching or mortality events[6]. Calcifying macroalgae are pivotal in driving ecosystem trajectories under present-day conditions, and their significance will only continue to grow with the global decline in coral cover[7] and the transition towards algal-dominated states. Yet, significant gaps remain in our understanding of calcifying macroalgal responses to the local and global stressors that are driving contemporary reef degradation[8,9]. These gaps include marine heatwaves (MHWs), which have emerged as principal drivers of ecological collapse on coral reefs globally[10].

Our understanding of calcifying macroalgal responses to MHWs remains limited, particularly in tropical systems, in contrast to chronic warming, for which physiological responses are better understood. Under chronic exposure, elevated temperatures can cause pigment loss, mortality, and reduced calcification and photosynthetic performance[11–14]. However, the effects of warming can also be neutral[15] or positive[16], suggesting variable but robust photosynthetic and calcification physiology in some taxa. Positive calcification responses may reflect temperature-driven increases in carbonate saturation state within the calcifying microenvironment, although empirical support remains limited and inconclusive[17]. Despite these insights, the physiological impacts of MHWs remain less well

Biological and Environmental Sciences and Engineering Division, King Abdullah University of Science and Technology, Thuwal, Saudi Arabia. [2]Present address: Marine Biology Department, Centre Scientifique de Monaco, Monaco, Monaco. [3]Present address: Institute for Geosciences, Johannes Gutenberg University, Mainz, Germany. ✉e-mail: ekrieger@centrescientifique.mc; maggie.johnson@kaust.edu.sa

constrained. The few available studies, largely from non-tropical systems, tend to report muted physiological responses[17–19]. Extrapolating these findings to tropical taxa is problematic, given the narrower thermal safety margins of these organisms[20]. Considering their importance in maintaining the structural integrity and ecological functioning of coral reefs, there is an urgent need to understand how tropical calcifying macroalgae respond to MHWs and which parameters may modulate their tolerance.

Organismal tolerance to MHWs reflects physiological responses to local ocean climate variability across seasonal and broad spatial scales. At seasonal scales, negative MHW impacts are often more pronounced in summer than in winter, reflecting the respectively smaller or larger thermal safety margins (i.e., difference between tolerable and experienced temperatures)[21]. At the same time, thermal tolerance can also be lower in winter than in summer due to seasonal acclimatization[21]. Similar patterns of sensitivity emerge across spatial scales. Tropical taxa generally live closer to their thermal maxima than extratropical ones and therefore tend to experience negative impacts earlier[20]. Comparable differences are seen within species ranges: populations from the warm-edge of a distribution are typically more vulnerable than those from the cold-edge[22]. Yet, while cold-edge populations may be more tolerant and can even benefit from an alleviation of cold stress during MHWs, they may also be thermally naïve and thus more sensitive[23].

In addition to variability at seasonal and large spatial scales, MHW tolerance is further shaped by fine-scale thermal fluctuations such as diurnal temperature cycles. High-frequency (i.e., daily) temperature variability can enhance thermal tolerance in many organisms by promoting phenotypic plasticity, conferring greater resilience than in organisms from more thermally stable environments[24,25]. While enhanced heat tolerance in corals from thermally variable environments has likely reduced MHW impacts in associated reef communities[24,26,27], it remains unclear whether other key functional groups, such as calcifying macroalgae, exhibit similar responses. Addressing this knowledge gap is important because responses are not uniform: the impact of thermal variability on MHW tolerance can also be neutral or even negative[26,28], with diverging outcomes likely hinging on the magnitude, amplitude, and frequency of the fluctuations experienced[27]. Different variability regimes may also reduce the experienced heat stress, by directly interacting with the MHW. Significant cooling at night, for example, can offer a period of respite and recovery from peak daytime temperatures[29] and tidal flushing of cooler water may directly reduce daily temperature extremes[30,31]. Conversely, heat stress may be exacerbated in scenarios that intensify daily temperature extremes or create overlap with extremes in other environmental drivers.

Tolerance to MHWs is not only shaped by the thermal regimes encountered by organisms, but also by the broader environmental background, which includes all other abiotic parameters such as salinity, oxygen, irradiance and nutrient availability. For photoautotrophic taxa, both light and nutrient availability are particularly important for organismal performance[32–35]. Light is pivotal because it provides the primary energy for photosynthesis and, in the MHW context, modulates heat-stress responses[36,37]. Stressful temperatures can inhibit the dark reactions of photosynthesis[38], leading to a potentially harmful accumulation of unused energy. MHW-induced stress can therefore be amplified when peak temperatures coincide with periods of high irradiance. Although the interplay between irradiance and heat-driven bleaching is well documented in corals[39], comparable work on other tropical calcifiers remains scarce, particularly with macroalgae. Evidence from temperate non-calcifying macroalgae suggests that low, rather than high, light reduces MHW tolerance by limiting energy reserves, thereby constraining coping mechanisms[40]. In calcifying macroalgae, interactions between irradiance and chronic thermal stress often appear more muted[15], but have nevertheless been implicated in bleaching (i.e., loss of photosynthetic pigments) and mortality in both tropical[41] and temperate algae[42]. Acute heat stress and irradiance intensity do not appear to interact strongly, although evidence remains limited to two temperate coralline algal species[43]. Targeted experiments are now required to understand the role of irradiance, including its timing relative to peak heat stress, in influencing thermal tolerance to acute heat stress in tropical calcifying macroalgae.

Despite their importance to the persistence of coral reefs, the responses of calcifying macroalgae to MHWs and the factors that shape them remain insufficiently characterized. Within this broad functional group, two lineages are significant at global scales. The green, articulated alga *Halimeda* contributes to sediment production, while crustose coralline algae (CCA) provide structural stability and facilitate coral recruitment. In this study, we assessed the tolerance of four calcifying reef-algal species from the Red Sea to a simulated MHW, using two representatives from each lineage. Specifically, we addressed knowledge gaps regarding the physiological responses of these important functional taxa to MHW exposure and examined how these responses are modulated by diurnal temperature variability. By applying two variability regimes that differed in peak-temperature timing (daytime versus nighttime), we further explored the potential mechanistic role of temperature–irradiance coupling. We predicted that (1) diurnal temperature variability would enhance macroalgal tolerance to an MHW, whereas (2) co-occurrence of the daily irradiance maximum with the temperature peak would reduce that tolerance.

Material and methods

Sample collection and field site

Algae were collected haphazardly by snorkelers one month (18th May 2023) prior to the start of the experiment (19th June 2023) at depths between 0.5 and 2 m on the Al-Fahal reef flat in the central Red Sea (22.297604, 38.962194). Based on qualitative field observations, the four selected species represent the most commonly encountered calcifying macroalgal taxa at the collection site Two crustose coralline algal species (*Lithophyllum* sp. and *Neogoniolithon* sp., $n = 120$ individuals per species) were collected from the reef flat as uniform (i.e., single species), free-living nodules. These species differ macro-morphologically, which facilitates field collections of the same species. For example, *Lithophyllum* sp. used in this study has branching protuberances, making it more structurally complex than the smooth, encrusting *Neogoniolithon* sp. Individuals of two *Halimeda* species (*H. opuntia* and *H. discoidea*, $n = 120$ individuals per species) were collected from cracks and crevices in the reef framework by carefully prying the holdfast loose from the substrate, while minimizing damage to the thallus. The two *Halimeda* species are morphologically distinct, with *H. discoidea* having larger and less calcified segments than *H. opuntia* (Fig. 1c).

After collection, algae were placed in coolers with seawater and transported immediately to the wet lab facilities at King Abdullah University of Science and Technology (KAUST). In the laboratory, organisms were carefully rinsed with seawater and cleaned of larger epibionts before being placed in experimental tanks. Algae were allowed to recover from collection for two days at 29 °C, with a daily light dose of ~2.6 mol m^{-2} d^{-1}. After this initial resting phase, temperatures were slowly increased over eight days (~0.35 °C d^{-1}) until the target baseline temperature (31.7 °C) was reached. During these 10 days of acclimation, the organisms were carefully cleaned of remaining epibionts and labeled with zip-tie tags. To prevent damage to fragile *Halimeda* segments, a piece of rubber tubing was placed between the thallus and the tag. After labeling and cleaning, algae were left in the tanks for another 10 days. After this period, the day and night temperatures were slowly raised or lowered (0.15 °C d^{-1}) over the course of an additional 10 days to create the desired diurnal variability (3 °C) in the respective treatments. Specimens (except for *H. discoidea*, which does not respond well to carbonate staining) were then stained with alizarin red (0.75 g L^{-1}) in resealable plastic bags for 24 h to mark pre-existing skeletal material for potential subsequent geochemical analyses. Organisms were then removed from the bag and initial response variables were measured, marking the start of the experimental treatments and the pre-MHW phase. The experiment ran for 70 days from the 19th of June to the 28th of August 2023. An overview of the experimental timeline is provided in Table 1.

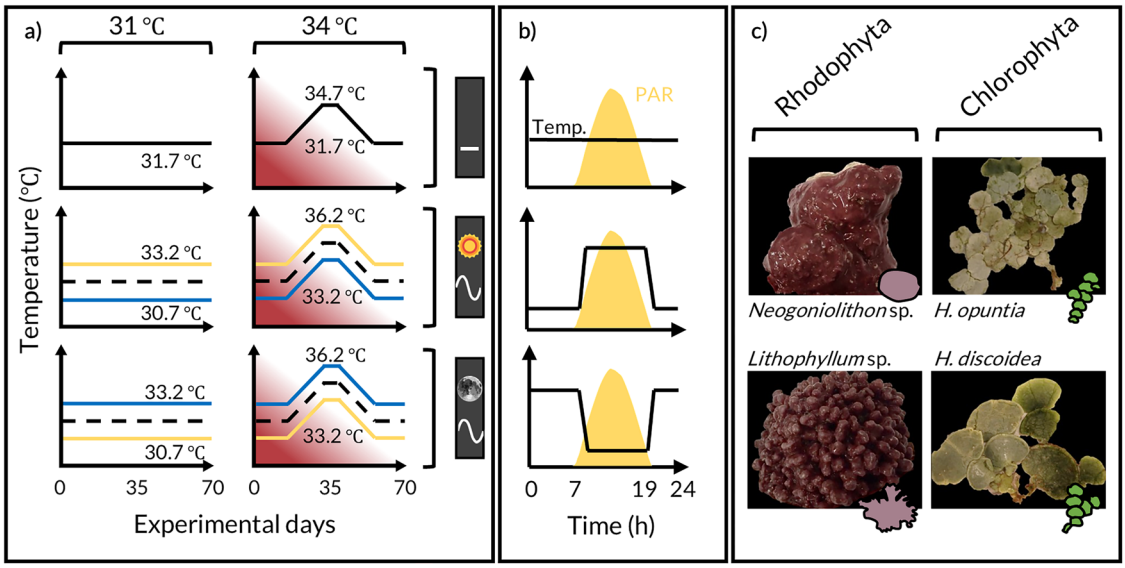


Fig. 1 | Experimental design and study species. a Schematic illustrating experimental design and treatments. Treatments with a red background were exposed to the heatwave, while those with a white background remained at normal summer temperatures. Temperatures in black text indicate target temperatures. Dashed and solid black lines indicate mean temperatures. Solid blue and yellow represent night and daytime temperatures, respectively. White straight and wavy lines indicate whether temperatures were stable or varied over the course of a day, respectively. The sun and moon symbols represent treatments with peak temperatures during the day and at night, respectively. **b** The relationship between photosynthetically active radiation (PAR) and temperature in the different treatments. **c** Pictures of the four species studied. Photos: Erik C. Krieger and Huajing Yan.

Taxonomic identification of coralline algae

The coralline algae collected for the experiment were identified using morpho-anatomical characteristics, although we acknowledge the known difficulties with this approach[44]. Macroscopic identification was verified by molecular analysis of prior collections of the same morphotypes from the same site, which revealed little to no cryptic diversity (Fig. S1). Thus, we are confident that our coralline algal samples consistently belong to two undescribed species, one in the genus *Lithophyllum* and one in the genus *Neogoniolithon*.

The full molecular protocols of this verification step are detailed in Giorgi et al.[45], with brief methodological details provided here for completeness. DNA was extracted from RNAlater™-preserved or air-dried fragments using the Qiagen Plant Mini Kit (Qiagen, Germantown, MD, USA). PCR amplification targeted the chloroplast rbcL gene using the forward primer F753 in combination with either RrbcS[46] or R1460cor[47], yielding amplicons of approximately 700–750 bp. PCR thermal cycling conditions followed[48]. Successful amplification and fragment size were verified by agarose gel electrophoresis prior to purification using the Omega Bio-Tek MicroElute Cycle Pure Kit (Omega Bio-Tek Inc., Norcross, GA, USA). Purified PCR products were bidirectionally sequenced at the KAUST Bioscience Core Lab, and sequence assembly and phylogenetic analyses followed Giorgi et al.[45], with genus identity confirmed based on placement within well-supported clades containing reference sequences.

Experimental treatments and design

The study was conducted in the aquarium facilities at KAUST's Coastal Marine Resources core lab, located on the central coast of the Saudi Arabian Red Sea, 30 min from the collection site. The experiment included six treatments combining two thermal regimes, control and MHW, with three variability conditions: (1) no temperature variability, (2) diurnal variability with peak temperatures during the day, and (3) diurnal variability with peak temperatures during the night (Fig. 1a). The baseline/non-MHW (i.e., control) temperature (31 °C) corresponded to the maximum monthly mean (30.93 °C) at the collection site (Fig. S2) while the selected diurnal variability of 3 °C exceeded the average daily temperature variation observed there (mean: 1.73 °C; Figs. S3–S4). We adjusted the baseline temperature of 31 °C upwards by 0.7 °C to account for the mean annual discrepancy between the satellite record and logger-based in situ measurements (Fig. S5). Thus, baseline temperatures and peak MHW intensity were closer to 31.7 °C and 34.7 °C, respectively (Fig. 1a and Table S1). Heatwave intensity and duration were modeled after regional historic MHWs, but it should be noted that simulated events are above average in terms of strength and duration (Fig. S6 and Tables S2–4).

Each treatment was replicated three times at the tank level for a total of eighteen tanks. However, one tank assigned to the control regime with daytime-peaking temperatures experienced a temperature-control failure at the start of the experiment. Samples from this tank were therefore excluded from all analyses. Each tank initially held five specimens of each species, but mortality prior to MHW exposure (i.e., the pre-MHW phase) decreased the number of replicates in the subsequent experimental phases (Table S5). In addition to the 90 initial individuals, we distributed 30 additional specimens for each of the two coralline algal species into the tanks (five per treatment). These samples were destructively sampled at the peak of the MHW for the Raman analysis (see section "Raman spectroscopy" below). All samples were placed on clear acrylic racks, elevated above the bottom of the tank to spatially separate them from the pumps and the heaters.

Experimental conditions

Seawater supply. Seawater was pumped from a depth of 5–6 m from 1.3 km offshore to an onshore intake facility at KAUST's core lab. At the facility, the seawater was filtered (20 µm sand filter) and temperature adjusted to 27 °C before being pumped into the individual 70 L flow-through tanks at a rate of 150 mL min^{-1}. Each tank contained a wavemaker pump (EcoDrift 4.3, AB Aqua Medic GmbH, Bissendorf, Germany) to facilitate circulation and mixing.

Temperature control. Temperature in the individual tanks was controlled using two submersible 600 W titanium heaters placed at the bottom of each tank and connected to an aquarium controller (T controller Twin, AB Aqua Medic GmbH, Germany). Controllers turned the heaters on or off whenever temperatures deviated by 0.3 °C from the set value. Temperature settings for tanks with diurnal variability were

Table. 1 | Experimental timeline and phases

Dates	Experimental period	Description
18 May 2023	Acclimation	Sample collection
18–20 May 2023		Two-day post-collection recovery in experimental tanks at 29 °C
21–29 May 2023		Temperature increased from 29 °C to the experimental baseline of 31.7 °C over eight days (0.35 °C d^{-1})
29 May–8 June 2023		Ten-day rest period at 31.7 °C
9 June–19 June 2023		Daytime and night-time temperatures in the four variability treatments were increased or decreased over ten days (0.15 °C d^{-1})
20 June–4 July 2023	pre-MHW	All organisms were exposed to a mean temperature of 31.7 °C; one-third experienced no temperature variability, one-third experienced daytime-peaking variability, and one-third experienced nighttime-peaking variability.
5 July–9 August 2023	MHW	Half of the organisms were exposed to the simulated MHW, while the previously established variability treatments were maintained.
10 August–28 August 2023	post-MHW	All organisms were returned to a mean temperature of 31.7 °C; one-third experienced no temperature variability, one-third experienced daytime-peaking variability, and one-third experienced night-time-peaking variability.

Date range and brief description of experimental periods.

changed manually every morning (07:30–08:00) and evening (19:30–20:00). This timing coincided with the onset and offset of the photoperiod, ensuring the target temperature peaks were strictly aligned with either the light or dark phase to test the interplay between thermal and irradiance stress. Temperatures were validated with a handheld thermometer (Fisherbrand Traceable Digital Thermometer, Thermo Fisher Scientific Inc., USA) before daily temperature setpoints were changed. Further temperature monitoring was achieved with temperature loggers (HOBO MX2202, Onset, USA; calibrated against Fisherbrand Traceable Digital Thermometer, Thermo Fisher Scientific Inc., USA) (results see Table S1 and Figs. S7–S8). One logger was placed in each tank one week after the start of the experiment.

Seawater carbonate chemistry. Seawater carbonate chemistry in each tank was monitored through discrete measurements of both dissolved inorganic carbon (DIC) and pH on the total scale (pH_T) (results see Table S6). Measurements spanned different times of the day, including at night and during each experimental period, to capture any potential short- and long-term variability of pH_T and DIC. Total pH was measured with a pH meter (Orion Star A329 equipped with Orion Ross pH/ATC triode 8107UWMMD, Thermo Fisher Scientific Inc., USA) calibrated with Tris/HCl buffers[49]. Water for DIC analysis was collected in clean 120 mL borosilicate bottles. After the collection, samples were poisoned with mercuric chloride ($HgCl_2$), and the bottles were then sealed with greased ground glass stoppers following Dickson et al.[49]. All water samples for DIC analysis were processed within three weeks of collection. Samples for DIC were analyzed on an AS-C3 DIC analyzer (LI-COR Inc., USA). Regular analysis ($n = 63$) of certified reference material (Batch 206 provided by A.G. Dickson lab) yielded DIC concentrations accurate to within 0.02 µmol kg^{-1} of the nominal value, with a precision of ± 2.47 µmol kg^{-1}.

Irradiance. Light was provided by 95 W LED panels (Radion XR15 G6, EcoTech LLC., USA) mounted above each tank. The panels followed a natural 12 h diel cycle, with irradiance gradually increasing from 07:00 until reaching peak intensity at 13:00, and then decreasing until "sunset" at 19:00. Peak intensity was set to 100–135 µmol m^{-2} s^{-1} for a daily dose of approximately 2.6 mol m^{-2} d^{-1} (results see Tables S7–S8 and Fig. S8). The chosen irradiance levels strike a balance between the high light that coralline algae experience on the reef flat at the time of collection and the much lower light that *Halimeda* receives beneath overhangs; overall, they approximate the conditions found in larger reef crevices (Table S9 and Fig. S9). Photosynthetically active radiation (PAR) levels were regularly checked using a handheld underwater PAR meter (Apogee MQ-510, Apogee Instruments Inc., USA) and light loggers (HOBO MX2202, Onset, USA), which were calibrated against the handheld meter and placed in each tank at the center of the acrylic plastic racks.

Physiological metrics

Net calcification. Net calcification rates were quantified using the buoyant weight technique[50]. Buoyant weights obtained at the start and end of each experimental period were converted to the dry weight of calcite (for coralline algae) and aragonite (for *Halimeda*). Net changes in weight between timepoints were then normalized for time (in days) and surface area (in cm^2, see Section "Surface area determination" for more details) to obtain net calcification rates. To ensure correct calculations, label weights obtained during the last weighing session at the end of the experiment were subtracted from all previously obtained weights.

Photochemical efficiency. Variable fluorescence (Fv) normalized to maximal fluorescence (Fm) of each sample was measured in the middle of each experimental period (experimental days 17, 35 and 58; Fig. 1a) to determine maximum photosynthetic efficiency (Fv/Fm). Measurements of Fv/Fm were taken with a red-light Pulse Amplitude Modulated fluorometer (Diving-PAM-II/R, Heinz Walz GmbH, Effeltrich, Germany) 30 min after the end of the photoperiod (ca. 19:30) and only when minimum fluorescence (Fo) was >120. The same settings were used for all taxa, as they yielded reliable results for all species (saturation light intensity = 12; gain = 2; damping = 3; measuring light intensity = 1; saturation pulse width = 0.8).

Rapid light curves. Rapid light curves (RLCs) were used to characterize algal photosynthetic activity by deriving three key parameters: maximum relative electron transport rate ($rETR_{max}$), light-use efficiency (α; initial slope of the curve), and minimum saturation irradiance (E_k). RLCs were conducted midway through each experimental phase (days 17, 35, and 58; Fig. 1a) between 12:00 and 14:00. Measurements were obtained from five individuals per species and treatment, including at least two independent treatment tanks. Individuals were exposed for 10 s to each of the six increasing PAR levels, ranging from 0 to 497 µmol photons m^{-2} s^{-1}. Determination of $rETR_{max}$, α and E_k followed[51] using non-linear models that were fitted to the data via least-squares error calculations.

Raman spectroscopy. Confocal Raman spectroscopy provides more detailed insight into calcification physiology and was applied to determine sample mineralogy and carbonate lattice properties. Mineralogy was determined from the presence and shape of two Raman peaks: the ν_1 carbonate peak (1080–1090 cm^{-1}), which indicates $CaCO_3$, and the ν_4 peak (700–720 cm^{-1}), whose shape differentiates aragonite (double peak) from calcite (single peak). The position of the ν_1 peak provides information on Mg content, whereas the full width at half maximum (FWHM)

Table. 2 | Significant physiological responses and effect magnitudes of the simulated marine heatwave

Driver	Metric	Species	Phase	Reference (mean ± SE)	Treatment (mean ± SE)	Effect	$F(df_1,df_2)$	*p* value
MHW	Calcification	*Neogoniolithon* sp.	pre-MHW	0.0827 ± 0.0136	0.1573 ± 0.0288	90% increase	$F(1, 11.932) = 7.6119$	0.02
	Calcification	*H. opuntia*	MHW	0.022 ± 0.011	−0.001 ± 0.013	>100% decrease	$F(1, 25) = 6.6033$	0.02
		Lithophyllum sp.		0.027 ± 0.015	−0.025 ± 0.015	>100% decrease	$F(1, 6.6259) = 10.2160$	0.03
	Fv/Fm	*Neogoniolithon* sp.		0.61 ± 0.01	0.49 ± 0.02	9% decrease	$F(1, 57) = 12.3112$	0.01
		Lithophyllum sp.		0.64 ± 0.01	0.58 ± 0.01	20% decrease	$F(1, 13.939) = 8.0424$	0.01
	rETRmax	*H. opuntia*		17.22 ± 6.08	5.63 ± 1.30	67% decrease	$F(1, 13.940) = 7.4478$	0.02
		Neogoniolithon sp.		18.37 ± 3.72	15.66 ± 4.73	15% decrease	$F(1, 13.479) = 5.2858$	0.04
	E_k	*H. opuntia*		131.25 ± 25.55	28.23 ± 9.86	79% decrease	$F(1, 22) = 27.394$	0.01
	FWHM	*Lithophyllum* sp.		0.72 ± 0.06	1.23 ± 0.06	71% increase	$F(1, 7.3086) = 22.8664$	0.002
	Calcification	*Neogoniolithon* sp.	post-MHW	−0.0687 ± 0.0134	−0.1195 ± 0.0191	74% decrease	$F(1, 63) = 7.2884$	0.01
	Fv/Fm	*Lithophyllum* sp.		0.66 ± 0.01	0.60 ± 0.02	9% decrease	$F(1, 13.785) = 5.6006$	0.03

Physiological responses associated with the simulated heatwave across experimental phases. Note: "Reference" represents the no-variability, non-MHW treatment, while "Treatment" represents the no-variability MHW treatment. During the pre- and post-MHW phases, mean temperatures were identical across treatments. Data were analyzed using linear mixed-effects models with two-sided Type III ANOVA.

of the ν_1 peak reflects carbonate lattice disorder and has been used to approximate calcifying-fluid saturation state (Ω_{CF}) in corals[52]. FWHM likely tracks Ω_{CF} in coralline algae[53,54] and can be expected to do so in *Halimeda*. However, given the lack of studies validating this approach in *Halimeda*, Raman analyses were restricted to coralline algae. A total of 30 samples per species (five per treatment) were collected midway through the MHW phase. These samples were placed in all tanks solely for this purpose at the start of the experiment, and their removal did not affect replication for all other physiological metrics. For each sample, we obtained and analyzed nine spectra (three from surface cells of three different growth margins). The rest of the sample preparation and analysis follows the protocol described in Krieger et al.[55], which is based on the procedures established by DeCarlo et al.[52] and the abiogenic calibrations for Mg of Perrin et al.[56]. Measurements were conducted on a WITec Apyron alpha 300AR+ Raman spectroscope (Oxford Instruments, UK) using a 532 nm laser, a long working distance objective (×50 magnification and 0.5 numerical aperture) and a 1800 mm^{-1} grating. Wavenumber calibration was achieved through the repeated analysis of a silicon substrate.

Surface area determination

Surface area for coralline samples was calculated using a dry weight-surface area relationship. The relationship for each coralline taxon was determined using a subset of specimens from the same species, collected during a previous experiment. Dry weight for each specimen was calculated from buoyant weight as described above (see Section "Net calcification"), and surface area was obtained from 3D scans (FARO Edge and ScanArm, FARO Inc., USA and Geomagic Wrap, Oqton Inc. USA). The equation from the linear regression relating dry weight to surface area was then used to calculate surface area of all samples in this experiment.

The surface area each *Halimeda* species was calculated as above, except that the dry weight-surface area relationship was derived from this study's samples, and the dry weight was determined by directly weighing silica-dried material, rather than by converting buoyant weight. This approach was chosen because the silica-dried samples, especially *H. opuntia*, lost several segments during storage and handling, which would have caused a large discrepancy between the dry weight calculated at the end of the experiment and the scanned surface area. Since samples were scanned from only one side, the measured surface area was doubled to estimate the total surface. Derived relationships for all species are shown in Fig. S10.

Statistical analysis

In accordance with our two initial research hypotheses, the statistical analysis was performed in two steps. In the first step, we analyzed the individual and interactive effects of the variability treatment and the MHW treatment with a linear mixed effect model using the whole dataset. In this first model (Model 1), variability, MHW and their interaction were included as fixed effects and tank identity as a random effect. Both fixed effects had two levels, with variability treated as a discrete ("YES" and "NO") and MHW as a continuous variable (31 °C and 34 °C). In the second step, we examined the role of temperature variability more closely by contrasting the two thermal regimes (i.e., temperature peaking at night or day) and their interaction with the MHW. To do so, we again employed a linear mixed effects model, but only with the data from the four variability treatments. The second model (Model 2) is identical to the one used in the first step of our analysis, except levels of variability were coded as "DAY" and "NIGHT" to reflect the occurrence of temperature peaks during the day or night, respectively. Normality and homoscedasticity were assessed using graphical analysis of residuals with the R package "sjPlot". Treatment effects were determined using one-way ANOVAs with *p*-values calculated using "lmerTest". Proportions of the variation (R^2) explained by the full models were calculated with the package "MuMin". We were unable to test interactions among drivers in the analysis of light-curved-derived photophysiological parameters of *H. opuntia* and *Neogoniolithon* sp., due to a smaller sample size during the post-MHW period. All analyses were conducted using R (version 4.3.1).

Results

Physiological outcomes associated with the MHW

Model 1 was applied to the pre-MHW phase to test for potential differences among experimental groups before the onset of the MHW treatment, when mean temperatures were still identical across treatments. Future MHW assignment had no significant effect on calcification, photochemical efficiency (Fv/Fm), maximum relative electron transport rate ($rETR_{max}$), saturation irradiance (*Ek*), or light-use efficiency (α) (Table 2 and Tables S10–S14), with one exception. *Neogoniolithon* sp. exhibited higher calcification in treatments assigned to the future MHW condition.

During the MHW phase, multiple responses were affected by heatwave exposure (Table 2 and Tables S15–S21). Calcification declined and became net negative in both *Lithophyllum* sp. and *H. opuntia*, whereas no significant change was detected in *Neogoniolithon* sp. or *H. discoidea* (Fig. 2). Fv/Fm decreased under MHW conditions but only in the two coralline algal taxa,

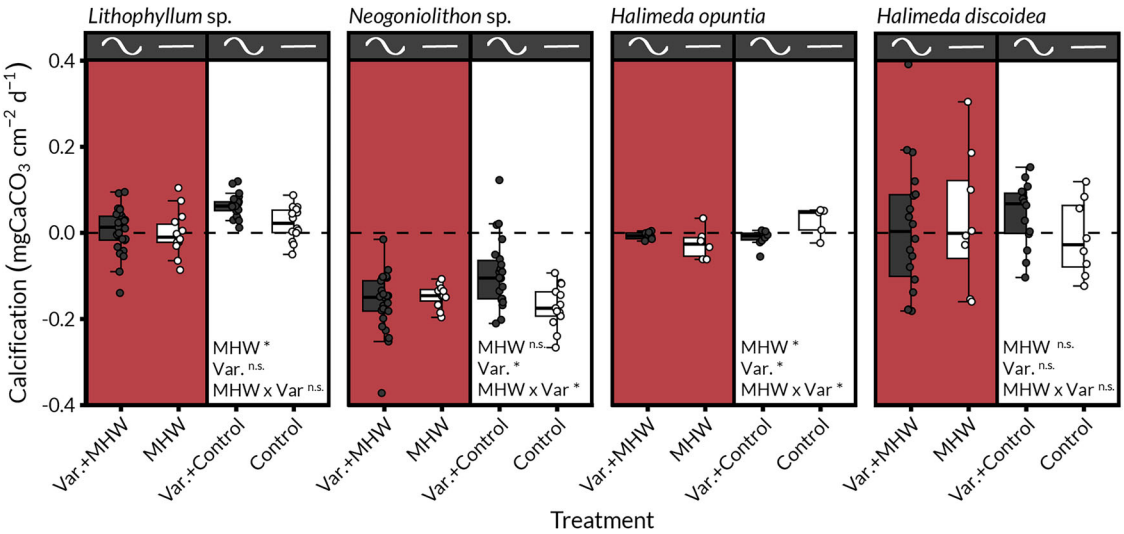


Fig. 2 | Calcification responses to the simulated marine heatwave and diurnal thermal variability. Calcification rates of the study species during the MHW phase, depending on exposure to normal (white plot background) or anomalous (red plot background) summer temperatures and thermal variability. Symbols above plots indicate treatments with (wavy line) or without thermal variability (straight line). Points show individual values. Solid line indicates the median, box shows the interquartile range (IQR) and the whiskers are 1.5×IQR. Species-specific sample sizes were: *Lithophyllum* sp. ($n = 79$), *Neogoniolithon* sp. ($n = 71$), *Halimeda opuntia* ($n = 29$), and *Halimeda discoidea* ($n = 48$).

Table 3 | Significant physiological responses and effect magnitudes of diurnal thermal variability

Driver	Metric	Species	Phase	Reference (mean ± SE)	Treatment (mean ± SE)	Effect	$F(df_1, df_2)$	*p* value
Diurnal variability	Calcification	*H. opuntia*	MHW	0.027 ± 0.015	−0.011 ± 0.006	>100% decrease	$F(1, 25) = 9.6079$	0.005
		Neogoniolithon sp.		−0.171 ± 0.014	−0.095 ± 0.017	44% increase	$F(1, 67) = 8.1509$	0.01
	Fv/Fm	*Lithophyllum* sp.		0.64 ± 0.01	0.58 ± 0.01	9% decrease	$F(1, 13.995) = 6.5267$	0.02
	E_k	*H. opuntia*		131.25 ± 25.55	75.17 ± 10.75	43% decrease	$F(1, 22) = 7.052$	0.01
		H. discoidea		76.28 ± 10.33	54.15 ± 6.02	32% decrease	$F(1, 26) = 16.4651$	0.0004
	Calcification	*Neogoniolithon* sp.	post-MHW	−0.0687 ± 0.0134	−0.0154 ± 0.0227	78% increase	$F(1, 63) = 5.9559$	0.02

Physiological responses associated with exposure to diurnal temperature variability across experimental phases. Note: "Reference" represents the stable (no-variability) treatment under non-MHW conditions, while "Treatment" represents the combined variable treatments (day- and night-peaking) under the same conditions. Data were analyzed using linear mixed-effects models with two-sided Type III ANOVA.

Lithophyllum sp. and *Neogoniolithon* sp. Electron transport was reduced under MHW exposure in *H. opuntia* and *Neogoniolithon* sp., but was not significantly affected in the other taxa. E^k was reduced only in *H. opuntia*, while α was unaffected across species.

Raman-derived skeletal metrics were assessed exclusively during the MHW phase and only in the two coralline taxa (Tables S20–S21). Magnesium content (% Mg) did not differ between treatments. However, full-width at half-maximum (FWHM) of the ν_1 carbonate peak increased in *Lithophyllum* sp. due to MHW exposure.

Following the five-week MHW phase, all treatments were returned to a common temperature for a two-week post-MHW recovery period. Residual effects of prior heat exposure were limited and confined to the coralline algae. Calcification in *Neogoniolithon* sp. was reduced following MHW exposure, despite no difference being detected in this species during the heatwave itself. In addition, Fv/Fm in *Lithophyllum* sp. remained suppressed during recovery. No other species or response variables differed between former MHW and non-MHW treatments during recovery (Tables S22–27).

Physiological impacts driven by exposure to diurnal temperature variability

All study organisms were exposed to one of three variability regimes (no variability, daytime-peaking, or nighttime-peaking) across all experimental phases, irrespective of MHW exposure. Model 1 evaluated the overall effect of diurnal variability by comparing the variable regimes against the stable (no-variability) treatments. Overall, diurnal variability exerted limited effects on physiology (Table 3 and Tables S10–S26). No significant responses were detected during the pre-MHW phase, and most effects were confined to the MHW phase.

During the MHW phase, variability resulted in a complete cessation of calcification in *H. opuntia*, while *Neogoniolithon* sp. exhibited higher calcification under variable conditions than under stable temperatures. This positive effect persisted into the recovery phase, representing the only significant variability-driven response during that period. Photophysiological responses during the MHW phase were predominantly negative. Fv/Fm declined in *Lithophyllum* sp. under variable conditions, while E^k was reduced in both *Halimeda* taxa.

Interactions between the simulated MHW and diurnal variability

Model 1 was used to assess interactions between the MHW and diurnal variability across all experimental phases (Table 4 and Tables S10–S26). Because mean temperatures were equal among treatments during the pre-MHW and recovery phases, significant interactions were largely restricted to the MHW phase. Where interactions were not additive, they were predominantly antagonistic, occurring with both positive and negative directionality.

In *H. opuntia*, both the MHW and thermal variability independently caused a complete cessation of calcification; however, their combined effect was weaker than expected from the sum of their individual effects, indicating negative antagonism. In contrast, *Neogoniolithon* sp. exhibited positive effects of both drivers on calcification, yet their interaction reduced the expected combined positive response, representing positive antagonism.

Photophysiological metrics showed similar non-additive responses. In *Lithophyllum* sp., both the MHW and variability reduced Fv/Fm, but a negative antagonistic interaction diminished their combined impact. In *H. opuntia*, E_k decreased under both stressors, yet their interaction reduced the magnitude of the combined decline, again indicating negative antagonism. Finally, in *H. discoidea*, E_k decreased under variability alone and was unaffected by the MHW; however, a positive synergistic interaction between the two drivers offset the expected negative impact, resulting in a net positive response under combined exposure.

Comparison of the two diurnal variability regimes

Model 2 was based on a reduced dataset that excluded the stable (no-variability) treatments and was used to explicitly compare the two variability regimes (day-peaking vs. night-peaking) and their respective interactions with the MHW (Fig. 3, Table 5, and Tables S27–S43). Across all experimental phases, only two significant differences between variability regimes were detected, both reflecting less favorable performance under nighttime temperature peaks.

In *H. opuntia*, pre-MHW calcification was significantly higher under the day-peaking than under the night-peaking regime. Similarly, light-use efficiency (α) in *Lithophyllum* sp. was significantly reduced when temperature peaks occurred at night.

Interactions of the two variability regimes with the MHW

The two thermal regimes generally did not interact with the MHW, with one exception (Table 6 and Tables S27–S43). In *H. opuntia*, pre-MHW calcification was higher under day-peaking variability, whereas treatments assigned to the future MHW exhibited slightly lower calcification; however, the combined effect of these drivers was weaker than expected under additivity, indicating positive antagonism.

Deviations in heatwave impact between tested models

Due to the design of Model 2, the model also tested for MHW effects, as well as differences between the two variability regimes and their interaction with the MHW. However, assessing overall heatwave impacts was not the primary aim of this model; therefore, interpretation of general MHW effects relies on Model 1 and the full dataset. As expected, most MHW responses identified in Model 1 were broadly confirmed, given the substantial overlap in data. Where deviations occurred, these are summarized below.

With respect to calcification, the negative heatwave effect over the MHW-phase in *H. opuntia* was no longer significant. Similarly, the heatwave-associated declines during the MHW-phase in Fv/Fm in *Lithophyllum* sp. and in $rETR_{max}$ in *H. opuntia* were not retained under Model 2. Conversely, α in *Lithophyllum* sp. was now significantly reduced during the MHW-phase under MHW conditions. Patterns regarding E^k also shifted slightly. Previously detected negative MHW effects in *Neogoniolithon* sp. and *H. opuntia* were not significant in Model 2, whereas in *H. discoidea* the MHW was associated with an increase in E^k during the MHW-phase. Finally, the positive MHW effect on FWHM in *Lithophyllum* sp. observed under Model 1 was not retained. In all remaining cases, Model 2 confirmed

Table. 4 | Significant physiological responses, effect magnitudes and interaction directionality of the simulated marine heatwave and diurnal thermal variability

Driver	Metric	Species	Phase	MHW (Δ)	Variability (Δ)	Expected (Δ)	Observed (Δ)	Deviation	Interaction type	$F(df_1,df_2)$	*p* value
MHW × variability	Calcification	*H. opuntia*	MHW	−0.052	−0.-038	−0.090	−0.034	89% weaker	Negative antagonism	$F(1, 25) = 9.3269$	0.01
		Neogoniolithon sp.		0.024	0.076	0.1	0.01	90% weaker	Positive antagonism	$F(1, 67) = 7.6491$	0.01
	Fv/Fm	*Lithophyllum* sp.		−0.060	−0.-060	−0.120	−0.060	50% weaker	Negative antagonism	$F(1, 13.939) = 6.0374$	0.03
	E_k	*H. opuntia*		−103.02	−56-.08	−159.10	−91.13	43% weaker	Negative antagonism	$F(1, 22) = 6.640$	0.02
		H. discoidea		−24.23	−22-.13	−46.36	6.35	114% stronger	Positive synergism	$F(1, 26) = 16.9558$	0.0003

Physiological responses associated with the interaction between diurnal temperature variability and the simulated heatwave across experimental phases. Effects (Δ) represent changes relative to the no-variability, no-MHW treatment. Expected additive effects were calculated as the sum of single-driver effects and compared with observed combined effects. Deviations from additivity were used to classify interactions as antagonistic or synergistic following Piggott et al.[74]. Data were analyzed using linear mixed-effects models with two-sided Type III ANOVA.

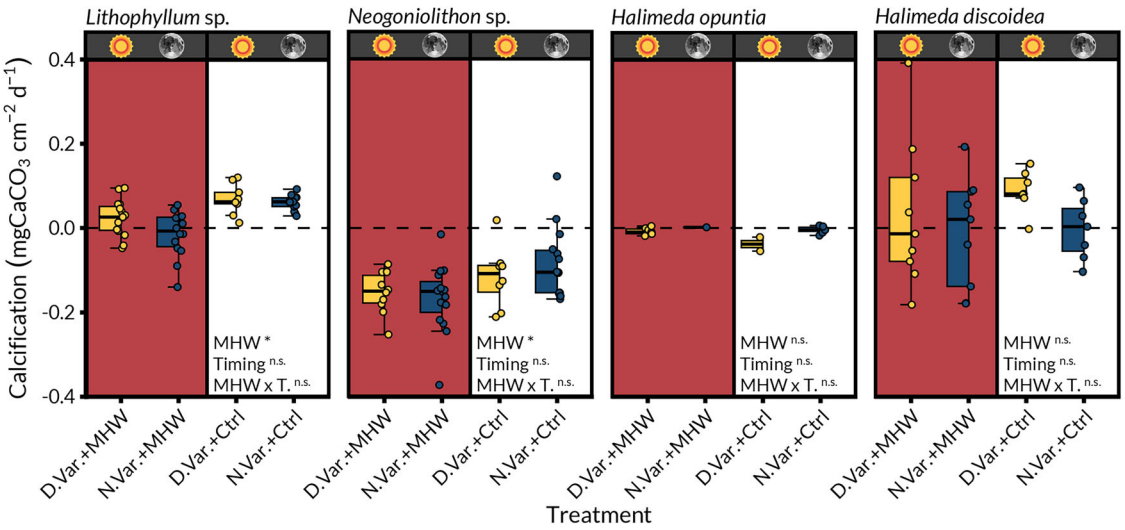


Fig. 3 | Calcification responses to the simulated marine heatwave and the timing of peak temperatures. Calcification rates of the study species during the MHW phase, depending on exposure to normal (white plot background) or anomalous (red plot background) summer temperatures, and across thermal variability regimes with different peak timing (day = yellow; night = blue). Symbols above the plots indicate treatments with elevated daytime (sun) or nighttime (moon) temperatures. Points show individual values. Solid line indicates the median, box shows the interquartile range (IQR) and the whiskers are 1.5×IQR. Species-specific sample sizes were: *Lithophyllum* sp. ($n = 51$), *Neogoniolithon* sp. ($n = 47$), *Halimeda opuntia* ($n = 18$), and *Halimeda discoidea* ($n = 32$).

Table. 5 | Significant physiological responses and effect magnitudes of peak temperature timing

Driver	Metric	Species	Phase	Reference (mean ± SE)	Treatment (mean ± SE)	Effect	$F(df_1,df_2)$	*p* value
Variability phase	Calcification	*H. opuntia*	pre-MHW	−0.2107 ± 0.0608	−0.4722 ± 0.0198	100% decrease	$F(1, 6.0994) = 8.4195$	0.03
	α	*Lithophyllum sp.*	MHW	0.39 ± 0.09	0.26 ± 0.02	33% decrease	$F(1, 17) = 4.5120$	0.049

Physiological responses associated with the timing of diurnal variability (day-peaking vs night-peaking) across experimental phases. Note: "Reference" represents the day-peaking variability treatment, while "Treatment" represents the night-peaking variability treatment. Effects are derived from comparisons under non-MHW conditions and presented for each experimental phase. Data were analyzed using linear mixed-effects models with two-sided Type III ANOVA.

the direction and significance (or lack thereof) of MHW effects identified in Model 1.

Discussion

Diurnal temperature variability exerted only a minor, inconsistent influence on the response of four tropical calcifying reef algae to a simulated MHW. We had posited that diel temperature fluctuations of 3 °C would bolster heatwave tolerance, yet significant MHW × variability interactions occurred in only five cases, with mixed effects on MHW impact. Variability mitigated MHW-driven reductions in calcification in *H. opuntia*, maximum quantum yield (Fv/Fm) in *Lithophyllum* sp. and light-saturation irradiance (E^k) in *H. opuntia* and *H. discoidea*, but it exacerbated the decrease in calcification in *Neogoniolithon* sp. Variability alone had an equally equivocal and limited influence, enhancing calcification in *Neogoniolithon* sp., but depressing calcification in *H. opuntia*, Fv/Fm in *Lithophyllum* sp., and E^k in *H. opuntia* and *H. discoidea*. The phase of the thermal cycle (day- versus night-peaking) produced few robust effects, although mean metabolic rates were generally higher when peak temperatures occurred during daylight. Indeed, the only significant diel-phase impacts, lower calcification in *H. opuntia* and reduced light-use efficiency (α) in *Lithophyllum* sp., were linked to elevated nighttime temperatures, the opposite of our a priori expectation. Across all treatments, the MHW itself was the dominant driver, suppressing calcification and photophysiological performance in *Neogoniolithon* sp., *Lithophyllum* sp. and *H. opuntia*. The muted and mixed contribution of short-term variability suggests that thermal limits in these algae are set primarily by long-term adaptation and acclimation, rather than by recent exposure to different variability regimes.

A limited capacity for our short-term exposure to differing variability regimes to enhance heat tolerance can be expected when long-term environmental history dominates thermal acclimatisation[27]. Although unanticipated, this is also not entirely unexpected here. The period during which the organisms experienced differing variability regimes was relatively short (14–24 d), and all samples originated from the same reef flat. Similar control by long-term history has been reported for *Phymatolithon lusitanicum*[19], where a short temperature pulse prior to the MHW nonetheless improved thermal resilience. In contrast, thermal priming had no or negative effects in three temperate macroalgae (*Sargassum linearifolium*, *Phyllospora comosa* and *Ecklonia radiata*)[57], and prolonged acclimation to warming reduced tolerance in *Porolithon cf. onkodes*[58]. In the temperate coralline alga *Ellisolandia elongata*, long- and short-term histories contributed equally to heat tolerance[59]. As is evident from these disparate study outcomes, environmental history has a highly variable influence on heat tolerance in marine macroalgae. But it should be noted that the aforementioned studies differ methodologically from each other and from this study. Indeed, only the present study examined the role of diurnal temperature variability. More studies are clearly needed to reconcile the differing results and further explore the role of environmental history and thermal variability in shaping MHW tolerance in marine macroalgae.

The MHW depressed metabolism in *Lithophyllum* sp., *Neogoniolithon* sp. and *H. opuntia*, suppressing both calcification and multiple photophysiological performance metrics. Calcification decreased in *H.*

Table. 6 | Significant physiological responses, effect magnitudes and interaction directionality of the simulated marine heatwave and peak temperature timing

Driver	Metric	Species	Phase	MHW (Δ)	Timing (Δ)	Expected (Δ)	Observed (Δ)	Deviation	Interaction type	$F(df_1,df_2)$	*p* value
MHW x Timing	Calcification	*H. opuntia*	pre-MHW	−0.0287	0.2615	0.2328	0.0412	82% weaker	Positive antagonism	$F(1, 6.1176) = 7.0531$	0.03

Physiological responses associated with the interaction between the timing of diurnal variability (day-peaking vs night-peaking) and the simulated MHW across experimental phases. Effects (Δ) represent changes relative to the night-peaking, non-MHW treatment. Expected additive effects were calculated as the sum of individual driver effects and compared with observed combined responses. Deviations from additivity were used to classify interactions as antagonistic or synergistic following Piggott et al.[76]. Data were analyzed using linear mixed-effects models with two-sided Type III ANOVA.

opuntia and *Lithophyllum* sp.; Fv/Fm declined in *Lithophyllum* sp. and *Neogoniolithon* sp.; and $rETR_{max}$ and E_k were lowered in *H. opuntia* and *Lithophyllum* sp. By contrast, FWHM (i.e., proxy for calcifying fluid saturation state) increased in *Lithophyllum* sp., which is counterintuitive, particularly given the reduction in calcification in this species. However, an elevation in FWHM can result from reduced calcification[17,55] and likewise signal physiological impairment. The results thus contrast with several recent studies that reported limited heatwave effects on calcified macroalgae[17–19,43]. However, most previous studies have focused on extra-tropical species, which typically do not live near their thermal maxima[20]. In this light, the higher MHW sensitivity of our study species is both logical and concerning. Calcifying reef algae, particularly coralline taxa, are often viewed as key buffers of reef carbonate production under climate change because they can rapidly colonize open substrate following coral mortality[60]. This putative role assumes that these algae possess high thermal tolerance, an inference drawn from field observations in which coral loss is accompanied by a compensatory rise in coralline algal cover that sustains carbonate production[6,61]. Our data challenge that assumption. The study species proved heat-wave sensitive, although they also demonstrated substantial post-stress recovery. Calcifying reef algae may therefore be vulnerable to short-term thermal extremes, yet also capable of rapid rebound. Further laboratory and field studies are essential for defining the bounds of this resilience, testing the transferability of our findings to complex natural settings, and quantifying community-level consequences, particularly whether opportunistic taxa not only replace corals but also other algae, with corresponding effects on reef diversity and functioning[62].

Physiological responses to diurnal temperature variation were generally weak and inconsistent. Only four significant effects were detected: one positive, higher calcification in *Neogoniolithon* sp., and three negative, lower calcification in *H. opuntia*, lower saturation irradiance (E_k) in *H. discoidea* and a reduced maximum quantum yield (Fv/Fm) in *Lithophyllum* sp. The limited impact may reflect the naturally variable thermal regime at the collection site, where daily amplitudes can range from 0.4 to 6.4 °C (mean 1.73 °C). Consequently, individuals are likely able to buffer both the absence of variability (≤0.3 °C amplitude in "constant" treatments) and the above-average amplitude imposed here (3 °C in "variable" treatments). A negative response to constant temperature might nonetheless have been expected as the organisms originate from a thermally variable environment, but shifts in mean temperature usually exert stronger physiological control than changes in variance[63,64]. Notably, all variability-related trends emerged only during and after the MHW phase. The additional 1.5 °C overlaid on the MHW probably pushed temperatures towards critical thresholds: lethal-temperature estimates (LT_{50}) for another *Halimeda* species (*H. tuna*) and another coralline alga (*Lithothamnion* sp.) from the collection site are 37.13 and 36.31 °C, respectively[65], whereas the MHW+variability treatments briefly reached 36.2 °C. Such excursions could explain the observed negative effects. The positive response, however, is more plausibly attributed to the synergy of high irradiance and temperature during daylight, which can stimulate metabolic activity[66].

Physiological responses differed little between the two diurnal-variability regimes; nevertheless, high daytime temperatures generally supported superior metabolic performance. To isolate the effect of the diel timing of peak temperature, we analyzed a reduced data set that included only the variability treatments. The analysis largely reproduced MHW effects and revealed few additional responses attributable to diel timing: just two significant effects were detected, both negative and both linked to high night-time temperatures (see below). We initially hypothesized that variability regimes peaking during daylight would be most deleterious during the MHW phase because heat stress can reduce carbon fixation, increasing non-utilized photon energy and production of reactive oxygen species (ROS)[37,38]. Consistent with this expectation, the combination of high daytime temperature and MHW yielded the lowest mean values of maximum relative electron transport rate ($rETR_{max}$), saturation irradiance (E_k) and light-use efficiency (α). The pattern was unequivocal in the two coralline algal taxa, but less consistent in *H. opuntia* and absent in *H. discoidea*. Given that

Halimeda specimens were mainly collected from shaded parts of the reef and the coralline algae from the sun-lit reef flat (Fig. and Table S8), the reverse outcome might have been expected. Regardless, trends in the data were not significant, likely due to low midday tank irradiance (100–135 μmol photons m^{-2} s^{-1}), which limited the buildup of harmful excitation pressure and may even have buffered overall MHW impacts across treatments. Because Fv/Fm was unaffected across all species, any decline in performance should be interpreted as transient down-regulation rather than permanent photodamage[67]. Moreover, modest photosynthetic depression did not translate into reduced calcification, indicating that the high-light/high-temperature combination still conferred a net benefit[66]. Indeed, across all species, response variables and experimental phases, performance was higher under high daytime than high nighttime temperatures in 58% of comparisons.

Exposure to elevated nighttime temperatures appeared to induce physiological stress, yet statistically significant effects were confined to two cases: reduced pre-MHW calcification in *H. opuntia* and lower light-utilization efficiency during the MHW phase in *Lithophyllum* sp. Several mechanisms may underlie these responses. In terrestrial plants, high night temperatures restrict photosynthate export, triggering end-product feedback that down-regulates daytime photosynthesis[68]. The electron-transport rates measured here did not show such down-regulation, perhaps because a concomitant rise in dark respiration may have prevented carbohydrate accumulation. While respiration was not measured and responses to thermal stress can be variable, including potential metabolic depression, nighttime respiration frequently increases with temperature[69]. If such an increase in respiration occurred, it likely posed additional challenges to the study taxa. In calcifying photoautotrophs, greater nocturnal CO_2 release can lower net night-time calcification by enhancing dissolution and may even drive net decalcification[70]. Across taxa, mean calcification was lower under high nighttime than high daytime temperatures in 68% of pairwise comparisons during the pre-MHW and MHW phases, but this difference vanished during recovery, suggesting physiological adjustment (e.g., reduced dark respiration) once the algae acclimated to the inverted diurnal regime (Fig. S10). Because calcification was integrated over 24 h, day- and night-time contributions cannot be distinguished, and both may have been influenced by elevated nocturnal metabolism. Energy depletion overnight could constrain daytime calcification, a process that is energetically costly[71], and high night temperatures might disrupt nocturnal repair of the photosynthetic apparatus[72], although the photophysiological metrics showed little evidence of such damage. Overall, however, elevated night-time temperatures triggered only weak, inconsistent stress. Although the day–night warming asymmetry[73] is more muted in the ocean, the strong nocturnal heat sensitivity seen in terrestrial plants suggests that marine photoautotrophs still warrant further study.

Conclusion

Diurnal temperature variability exerted only a minor influence on tolerance to MHWs in four tropical calcifying macroalgae. Thermal limits are thus assumed to be governed chiefly by long-term acclimatization or adaptation rather than by the short-term variability regimes applied here. MHW exposure suppressed calcification and photosynthetic performance in *Lithophyllum* sp., *Neogoniolithon* sp., and *H. opuntia*, whereas *H. discoidea* was unaffected. Most impairments resolved during the post-heatwave recovery phase, indicating the potential for resilience following MHW exposure. Diurnal variability itself elicited only weak and inconsistent physiological responses, suggesting that these algae can cope with the range of temperature fluctuations experienced in situ. Elevated night-time temperatures tended to impose greater stress than daytime warming, yet effects were inconsistent and largely non-significant. Several priorities for future research emerge from this study. Given the pronounced sensitivity of terrestrial plants to nocturnal heat stress, impacts on aquatic photoautotrophs merit urgent investigation. Future studies should also aim to disentangle the relative contributions of recent thermal exposure, longer-term environmental history, and thermal variability to thermal limits in reef-associated macroalgae and to quantify MHW effects across a broader suite of taxa. Such knowledge is essential for predicting the ecological trajectories of tropical reef systems in the rapidly warming ocean.

Reporting Summary

Further information on research design is available in the Nature Portfolio Reporting Summary linked to this article.

Data availability

The datasets generated and analyzed during the current study are available in the Dryad Digital Repository (https://doi.org/10.5061/dryad.2v6wwq053). The data underlying the main figures are included within this repository.

Received: 18 September 2025; Accepted: 14 September 2026;
Published online: 29 September 2026

References

1. Teichert, S., Steinbauer, M. & Kiessling, W. A possible link between coral reef success, crustose coralline algae and the evolution of herbivory. *Sci. Rep.* **10**, 17748 (2020).
2. Weiss, A. & Martindale, R. C. Crustose coralline algae increased framework and diversity on ancient coral reefs. *PLoS ONE* **12**, e0181637 (2017).
3. Björk, M., Mohammed, S., Björklund, M. & Semesi, A. Coralline algae, important coral-reef builders threatened by pollution. *Ambio* **24**, 502–505 (1995).
4. Morse, A. N. C. & Morse, D. E. Flypapers for coral and other planktonic larvae: new materials incorporate morphogens for applications in research, restoration, aquaculture, and medicine. *BioScience* **46**, 254–262 (1996).
5. Littler, M. M. & Littler, D. S. The nature of crustose coralline algae and their interactions on reefs. in *Research and discoveries: the revolution of science through scuba* (eds Lang, M. A., Marinelli, R. L., Roberts, S. J. & Taylor, P. R.) 199–212 (Smithsonian Institution Press, 2013).
6. Cornwall, C. E. et al. Crustose coralline algae can contribute more than corals to coral reef carbonate production. *Commun. Earth Environ.* **4**, 105 (2023).
7. Eddy, T. D. et al. Global decline in capacity of coral reefs to provide ecosystem services. *One Earth* **4**, 1278–1285 (2021).
8. Silbiger, N. J. et al. Nutrient pollution disrupts key ecosystem functions on coral reefs. *Proc. R. Soc. B* **285**, 20172718 (2018).
9. Roberts, C. Effects of fishing on the ecosystem structure of coral reefs. *Conserv. Biol.* **9**, 988–995 (1995).
10. Hughes, T. P. et al. Spatial and temporal patterns of mass bleaching of corals in the Anthropocene. *Science* **359**, 80–83 (2018).
11. Webster, N. S., Soo, R., Cobb, R. & Negri, A. P. Elevated seawater temperature causes a microbial shift on crustose coralline algae with implications for the recruitment of coral larvae. *ISME J.* **5**, 759–770 (2011).
12. Anthony, K. R. N., Kline, D. I., Diaz-Pulido, G., Dove, S. & Hoegh-Guldberg, O. Ocean acidification causes bleaching and productivity loss in coral reef builders. *Proc. Natl. Acad. Sci. USA* **105**, 17442–17446 (2008).
13. Tanaka, Y., Suzuki, A. & Sakai, K. Effects of elevated seawater temperature and phosphate enrichment on the crustose coralline alga *Porolithon onkodes* (Rhodophyta). *Phycol. Res.* **65**, 51–57 (2017).
14. Buapet, P. & Sinutok, S. Physiological responses to increased temperature and irradiance in the calcifying macroalgae, *Halimeda macroloba*, *Halimeda opuntia* and *Padina boryana*. Appl. Ecol. *Environ. Res.* **21**, 4745–4780 (2023).
15. Comeau, S., Carpenter, R. C. & Edmunds, P. J. Effects of irradiance on the response of the coral Acropora pulchra and the calcifying alga *Hydrolithon reinboldii* to temperature elevation and ocean acidification. *J. Exp. Mar. Biol. Ecol.* **453**, 28–35 (2014).

16. Steller, D. L., Hernandez-Ayón, J. M., Riosmena-Rodríguez, R. & Cabello-Pasini, A. Effect of temperature on photosynthesis, growth and calcification rates of the free-living coralline alga *Lithophyllum margaritae*. *Cienc. Mar.* **33**, 441–456 (2007).
17. Krieger, E. C. et al. Tolerance of coralline algae to ocean warming and marine heatwaves. *PLoS Clim.* **2**, e0000092 (2023).
18. Rendina, F. et al. Physiological response of the coralline alga *Corallina officinalis* L. to both predicted long-term increases in temperature and short-term heatwave events. *Mar. Environ. Res.* **150**, 104764 (2019).
19. Schubert, N., Santos, R. & Silva, J. Living in a fluctuating environment increases tolerance to marine heatwaves in the free-living coralline alga *Phymatolithon lusitanicum*. *Front. Mar. Sci.* **8**, 791422 (2021).
20. Vinagre, C. et al. Vulnerability to climate warming and acclimation capacity of tropical and temperate coastal organisms. *Ecol. Indic.* **62**, 317–327 (2016).
21. Atkinson, J., King, N. G., Wilmes, S. B. & Moore, P. J. Summer and winter marine heatwaves favor an invasive over native seaweeds. *J. Phycol.* **56**, 1591–1600 (2020).
22. Smale, D. A. et al. Marine heatwaves threaten global biodiversity and the provision of ecosystem services. *Nat. Clim. Change* **9**, 306–312 (2019).
23. Hughes, T. P. et al. Emergent properties in the responses of tropical corals to recurrent climate extremes. *Curr. Biol.* **31**, 5393–5399.e3 (2021).
24. Safaie, A. et al. High frequency temperature variability reduces the risk of coral bleaching. *Nat. Commun.* **9**, 1671 (2018).
25. Schaum, C.-E., Buckling, A., Smirnoff, N. & Yvon-Durocher, G. Evolution of thermal tolerance and phenotypic plasticity under rapid and slow temperature fluctuations. *Proc. R. Soc. B* **289**, 20220834 (2022).
26. Klepac, C. N. & Barshis, D. J. Reduced thermal tolerance of massive coral species in a highly variable environment. *Proc. R. Soc. B* **287**, 20201379 (2020).
27. Schoepf, V., Sanderson, H. & Larcombe, E. Coral heat tolerance under variable temperatures: effects of different variability regimes and past environmental history vs. current exposure. *Limnol. Oceanogr.* **67**, 404–418 (2022).
28. Putnam, H. M. & Edmunds, P. J. The physiological response of reef corals to diel fluctuations in seawater temperature. *J. Exp. Mar. Biol. Ecol.* **396**, 216–223 (2011).
29. Richards, Z. T. et al. A tropical Australian refuge for photosymbiotic benthic fauna. *Coral Reefs* **38**, 669–676 (2019).
30. Hsu, P.-C. et al. Tide-induced periodic sea surface temperature drops in the coral reef area of Nanwan Bay, southern Taiwan. *J. Geophys. Res. Oceans* **125**, e2019JC015226 (2020).
31. Green, R. H., Lowe, R. J., Buckley, M. L., Foster, T. & Gilmour, J. P. Physical mechanisms influencing localized patterns of temperature variability and coral bleaching within a system of reef atolls. *Coral Reefs* **38**, 759–771 (2019).
32. Wiedenmann, J. et al. Nutrient enrichment can increase the susceptibility of reef corals to bleaching. *Nat. Clim. Change* **3**, 160–164 (2013).
33. Mayfield, A. B. & Gates, R. D. Osmoregulation in anthozoan–dinoflagellate symbiosis. *Comp. Biochem. Physiol. A* **147**, 1–10 (2007).
34. Alderdice, R. et al. Deoxygenation lowers the thermal threshold of coral bleaching. *Sci. Rep.* **12**, 18273 (2022).
35. Fernández, P. A. et al. Nitrogen sufficiency enhances thermal tolerance in habitat-forming kelp: implications for acclimation under thermal stress. *Sci. Rep.* **10**, 3186 (2020).
36. Sharkey, T. D. Effects of moderate heat stress on photosynthesis. *Plant Cell Environ.* **28**, 269–277 (2005).
37. Salvucci, M. E. & Crafts-Brandner, S. J. Inhibition of photosynthesis by heat stress. *Physiol. Plant.* **120**, 179–186 (2004).
38. Biswal, B. et al. Photosynthesis, a global sensor of environmental stress. *Curr. Sci.* **101**, 47–56 (2011).
39. Lesser, M. P. Irradiance dependency of oxidative stress and coral bleaching. *Coral Reefs* **43**, 1393–1403 (2024).
40. Tait, L. W. et al. Loss of giant kelp driven by marine heatwaves. *Front. Mar. Sci.* **8**, 638377 (2021).
41. Diaz-Pulido, G., Anthony, K. R. N., Kline, D. I., Dove, S. & Hoegh-Guldberg, O. Interactions between ocean acidification and warming on the mortality and dissolution of coralline algae. *J. Phycol.* **48**, 32–39 (2012).
42. Martone, P. T., Alyono, M. & Stites, S. Bleaching of an intertidal coralline alga: untangling the effects of light, temperature, and desiccation. *Mar. Ecol. Prog. Ser.* **416**, 57–67 (2010).
43. Krieger, E. C. et al. Tolerance of three temperate macroalgal taxa to marine heatwaves of differing durations and intensities is not modulated by irradiance. *Phycologia* **62**, 627–636 (2023).
44. Twist, B. A. et al. The need to employ reliable and reproducible species identifications in coralline algal research. *Mar. Ecol. Prog. Ser.* **654**, 225–231 (2020).
45. Giorgi, A. et al. DNA sequencing reveals higher taxonomic diversity of coralline algae (*Corallinales* and *Hapalidiales*, Rhodophyta) in the tropical western North Atlantic that complicates ecological studies. *Bot. Mar.* **67**, 561–586 (2024).
46. Rueness, J. Phylogenetic relationships of some European *Gelidium* (*Gelidiales*, Rhodophyta) species, based on rbcL nucleotide sequence analysis. *Phycologia* **33**, 187–194 (1994).
47. Hernandez-Kantun, J. et al. Reassessment of branched *Lithophyllum* spp. (*Corallinales*, Rhodophyta) in the Caribbean Sea with global implications. *Phycologia* **55**, 619–639 (2016).
48. Hughey, J. R., Silva, P. C. & Hommersand, M. H. Solving taxonomic and nomenclatural problems in Pacific *Gigartinaceae* (Rhodophyta) using DNA from type material. *J. Phycol.* **37**, 1091–1109 (2001).
49. Dickson, A. G., Sabine, C. L. & Christian, J. R. (eds). *Guide to Best Practices for Ocean CO_2 Measurements*. (PICES Special Publication, 2007).
50. Jokiel, P. L., Maragos, J. E. & Franzisket, L. Coral growth: buoyant weight technique. in *Coral Reefs: Research Methods* (eds Stoddart, D. R. & Johannes, R. E.) 529–541 (UNESCO 1978).
51. Walsby, A. E. Numerical integration of phytoplankton photosynthesis through time and depth in a water column. *N. Phytol.* **136**, 189–209 (1997).
52. DeCarlo, T. M. et al. Coral calcifying fluid aragonite saturation states derived from Raman spectroscopy. *Biogeosciences* **14**, 5253–5269 (2017).
53. DeCarlo, T. M. et al. Investigating marine bio-calcification mechanisms in a changing ocean with in vivo and high-resolution ex vivo Raman spectroscopy. *Glob. Change Biol.* **25**, 1877–1888 (2019).
54. Comeau, S., Cornwall, C. E., DeCarlo, T. M., Krieger, E. & McCulloch, M. T. Similar controls on calcification under ocean acidification across unrelated coral reef taxa. *Glob. Change Biol.* **24**, 4857–4868 (2018).
55. Krieger, E. C. et al. The role of irradiance in controlling coralline algal calcification. *Limnol. Oceanogr.* **68**, 1269–1284 (2023).
56. Perrin, J. et al. Raman characterization of synthetic magnesian calcites. *Am. Mineral.* **101**, 2525–2538 (2016).
57. Filbee-Dexter, K., Feehan, C. J. & Wernberg, T. Persistence of seaweed forests in the Anthropocene will depend on warming and marine heatwave profiles. *J. Phycol.* **59**, 679–690 (2023).
58. Page, T. M., Bergstrom, E. & Diaz-Pulido, G. Acclimation history of elevated temperature reduces the tolerance of coralline algae to additional acute thermal stress. *Front. Mar. Sci.* **8**, 655858 (2021).
59. McCoy, S. J. & Widdicombe, S. Thermal plasticity is independent of environmental history in an intertidal seaweed. *Ecol. Evol.* **9**, 13402–13412 (2019).

60. Cornwall, C. E. et al. Global declines in coral reef calcium carbonate production under ocean acidification and warming. *Proc. Natl. Acad. Sci. USA* **118**, e2015265118 (2021).
61. Fox, M. D. et al. Limited coral mortality following acute thermal stress and widespread bleaching on Palmyra Atoll, central Pacific. *Coral Reefs* **38**, 701–712 (2019).
62. Abdul Wahab, M. A. et al. Hierarchical settlement behaviours of coral larvae to common coralline algae. *Sci. Rep.* **13**, 5795 (2023).
63. Smale, D. A. Impacts of ocean warming on kelp forest ecosystems. *N. Phytol.* **225**, 1447–1454 (2020).
64. Fulton, C. J. et al. Sea temperature shapes seasonal fluctuations in seaweed biomass within the Ningaloo coral reef ecosystem. *Limnol. Oceanogr.* **59**, 156–166 (2014).
65. Anton, A. et al. Differential thermal tolerance between algae and corals may trigger the proliferation of algae in coral reefs. *Glob. Change Biol.* **26**, 4316–4327 (2020).
66. Ross, C. L. et al. Coral calcification mechanisms in a warming ocean and the interactive effects of temperature and light. *Commun. Earth Environ.* **3**, 72 (2022).
67. Burdett, H. L. et al. Dynamic photoinhibition exhibited by red coralline algae in the Red Sea. *BMC Plant Biol.* **14**, 139 (2014).
68. Tombesi, S. et al. Relationship among night temperature, carbohydrate translocation and inhibition of grapevine leaf photosynthesis. *Environ. Exp. Bot.* **157**, 293–298 (2019).
69. Martin, S., Castets, M.-D. & Clavier, J. Primary production, respiration and calcification of the temperate free-living coralline alga *Lithothamnion corallioides*. *Aquat. Bot.* **85**, 121–128 (2006).
70. Comeau, S., Carpenter, R. C. & Edmunds, P. J. Coral reef calcifiers buffer their response to ocean acidification using both bicarbonate and carbonate. *Proc. R. Soc. B* **280**, 20122374 (2013).
71. Cohen, A. L. & Holcomb, M. Why corals care about ocean acidification: uncovering the mechanism. *Oceanography* **22**, 118–127 (2009).
72. Li, G., Woroch, A. D., Donaher, N. A., Cockshutt, A. M. & Campbell, D. A. A hard day's night: diatoms continue recycling photosystem II in the dark. *Front. Mar. Sci.* **3**, 218 (2016).
73. Gaston, K. J., Gardner, A. S. & Cox, D. T. C. Anthropogenic changes to the nighttime environment. *BioScience* **73**, 280–290 (2023).
74. Piggott, J. J., Townsend, C. R. & Matthaei, C. D. Reconceptualizing synergism and antagonism among multiple stressors. *Ecol. Evol.* **5**, 1538–1547 (2015).

Acknowledgements

We thank Lucia R. Bravo, Ghalih Althagafi and Ethraa Alshareef for their help with the data collection; Abel Cortada Galvao for his help analyzing water samples for DIC and TA, preparing the samples for Raman spectroscopy and conducting the laser scans of the *Halimeda* specimens; the team of the Coastal and Marine Resources Core Lab for their help and support with the experiment and the boat captains for their help with sample collections and logger deployments.

Author contributions

E.C.K. and M.D.J. designed the research. E.C.K. wrote the paper. E.C.K., L.T., F.C.B., L.L., G.M. and H.Y. ran the experiment. W.R. provided environmental data that informed study design and experimental parameters. E.C.K. performed the statistical analysis. All authors edited the manuscript, or provided intellectual input, and agreed to its submission.

Funding

Funding for this study was provided by a KAUST Opportunity Fund Project (OFP-5541) and KAUST baseline research support awarded to MDJ.

Competing interests

The authors declare no competing interests.

Additional information

Supplementary information The online version contains supplementary material available at https://doi.org/10.1038/s42003-026-11053-7.

Correspondence and requests for materials should be addressed to Erik C. Krieger or Maggie D. Johnson.

Peer review information *Communications Biology* thanks all reviewer(s) for their contribution to the peer review of this work. Primary Handling Editors: Linn Hoffmann and Michele Repetto. A peer review file is available.

Reprints and permissions information is available at http://www.nature.com/reprints

Publisher's note Springer Nature remains neutral with regard to jurisdictional claims in published maps and institutional affiliations.

Open Access This article is licensed under a Creative Commons Attribution 4.0 International License, which permits use, sharing, adaptation, distribution and reproduction in any medium or format, as long as you give appropriate credit to the original author(s) and the source, provide a link to the Creative Commons licence, and indicate if changes were made. The images or other third party material in this article are included in the article's Creative Commons licence, unless indicated otherwise in a credit line to the material. If material is not included in the article's Creative Commons licence and your intended use is not permitted by statutory regulation or exceeds the permitted use, you will need to obtain permission directly from the copyright holder. To view a copy of this licence, visit http://creativecommons.org/licenses/by/4.0/.

© The Author(s) 2026

This Article in Press is shared early to give you faster access to new research. It is citable and carries a permanent DOI. The final edited version will replace it automatically.